THE JOURNAL OF PHYSICAL CHEMISTRY Letters

Letter

Cite This: J. Phys. Chem. Lett. 2019, 10, 925−935

pubs.acs.org/JPCL

Diagrammatic Coupled Cluster Monte Carlo

Charles J. C. Scott,*[,†] Roberto Di Remigio,*[,‡,¶] T. Daniel Crawford,[¶] and Alex J. W. Thom[†]

[†]Department of Chemistry, University of Cambridge, Cambridge CB2 1TN, United Kingdom

[‡]Hylleraas Centre for Quantum Molecular Sciences, Department of Chemistry, University of Tromsø - The Arctic University of Norway, N-9037 Tromsø, Norway

[¶]Department of Chemistry, Virginia Tech, Blacksburg, Virginia 24061, United States

ABSTRACT: We propose a modified coupled cluster Monte Carlo algorithm that stochastically samples connected terms within the truncated Baker−Campbell−Hausdorff expansion of the similarity-transformed Hamiltonian by construction of coupled cluster diagrams on the fly. Our new approach—diagCCMC—allows propagation to be performed using only the connected components of the similarity-transformed Hamiltonian, greatly reducing the memory cost associated with the stochastic solution of the coupled cluster equations. We show that for perfectly local, noninteracting systems diagCCMC is able to represent the coupled cluster wavefunction with a memory cost that scales linearly with system size. The favorable memory cost is observed with the only assumption of fixed stochastic granularity and is valid for arbitrary levels of coupled cluster theory. Significant reduction in memory cost is also shown to smoothly appear with dissociation of a finite chain of helium atoms. This approach is also shown not to break down in the presence of strong correlation through the example of a stretched nitrogen molecule. Our novel methodology moves the theoretical basis of coupled cluster Monte Carlo closer to deterministic approaches.

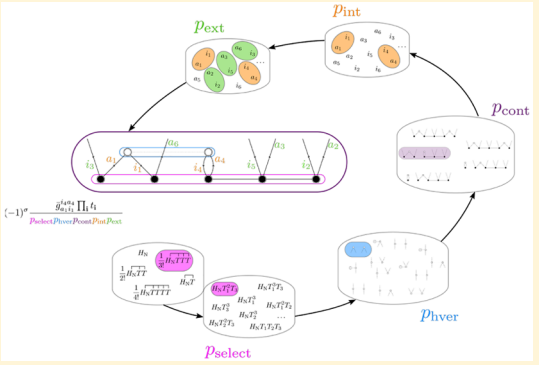

Over the last half-century, the coupled cluster (CC) wavefunction Ansatz has proved remarkably effective at representing the solution of the Schrödinger equation in a polynomial scaling number of parameters while providing size-extensive and -consistent results. Despite reducing the full configuration interaction (FCI) $N!$ factorial scaling to polynomial, the computational cost of CC methods, measured in terms of both required CPU floating-point operations and memory, is still an issue. The CC with single and double substitutions (CCSD) and CCSD with perturbative triples correction (CCSD(T)) approximations provide a balance between computational cost and accuracy that has led to relatively wide adoption but are eventually precluded for many large systems.

Recent work has made great progress on this issue through application of various approximations, which enable calculations to be performed with reduced memory and computational costs. In particular, various approximations exploiting the locality of electron correlation allow calculations with costs asymptotically proportional to measures of system size. These include approaches based on orbital localization,[1−38] molecular fragmentation,[39−51] and decompositions, such as resolution-of-the-identity, Cholesky, or singular-value of the two-electron integrals tensors.[19,20,52−57] However, while providing large efficiencies in CCSD calculations, higher truncation levels will generally exceed available memory resources before such approximations are a reasonable proposition.

In this Letter, we propose and demonstrate a CC-based projector Monte Carlo (MC) algorithm that enables automatic exploitation of the wavefunction sparsity for arbitrary excitation orders. Our methodology can be particularly beneficial for localized representations of the wavefunction, but it is not limited by assumptions of locality. The approach can fully leverage the sparsity inherent in the CC amplitudes at higher excitation levels,[58] allowing dramatic reductions in memory costs for higher levels of theory.

The CC wavefunction is expressed as an exponential transformation of a reference single-determinant wavefunction $|D_0\rangle$

$$|\mathrm{CC}\rangle = \mathrm{e}^{T}|D_0\rangle \tag{1}$$

where the cluster operator T is given as a sum of second-quantized excitation operators:

$$T = \sum_{k} T_k \tag{2}$$

with the kth order cluster operators expressed as sums of excitation operators weighted by the corresponding cluster amplitudes

$$T_k = \sum_{\mathbf{i}\in k\text{th replacements}} t_{\mathbf{i}}\tau_{\mathbf{i}} = \frac{1}{(k!)^2}\sum_{\substack{a_1,a_2,\ldots,a_k\\ i_1,i_2,\ldots,i_k}} t^{i_1 i_2 \ldots i_k}_{a_1 a_2 \ldots a_k}\tau^{a_1 a_2 \ldots a_k}_{i_1 i_2 \ldots i_k} \tag{3}$$

Received: January 9, 2019
Accepted: February 6, 2019
Published: February 6, 2019

DOI: 10.1021/acs.jpclett.9b00067
J. Phys. Chem. Lett. 2019, 10, 925−935

in the tensor notation for second quantization proposed by Kutzelnigg and Mukherjee.[59] Upon truncation of the cluster operator to a certain excitation level l and projection of the Schrödinger equation onto the corresponding excitation manifold, one obtains the linked energy and cluster amplitude equations

$$\langle D_0|\bar{H}_N|D_0\rangle = E_{CC} \tag{4a}$$

$$\Omega_{\mathbf{n}}(\boldsymbol{t}) = \langle D_{\mathbf{n}}|\bar{H}_N|D_0\rangle = 0 \tag{4b}$$

We have introduced the similarity-transformed Hamiltonian, $\bar{H}_N = e^{-T}H_N e^{T}$, and $|D_{\mathbf{n}}\rangle$ can be any state within the projection manifold (up to an l-fold excitation of $|D_0\rangle$). These CC equations are manifestly size-extensive order-by-order and term-by-term and furthermore provide the basis for the formulation of response theory.[60]

CC methods have to be carefully derived order-by-order and their implementation subsequently carried out, a process that can be rather time-consuming and error-prone.[61−63] It has long been recognized that the use of normal-ordering,[64,65] Wick's theorem[66] and the ensuing diagrammatic techniques[67] can be leveraged to automate both steps,[64,68−74] though spin-adaptation can still pose significant challenges.[75−77] Consider the normal-ordered, electronic Hamiltonian

$$\begin{aligned} H_N = F + \Phi &= \sum_{pq} f^q_p e^p_q + \frac{1}{2}\sum_{pqrs} g^{rs}_{pq} e^{pq}_{rs} \\ &= \sum_{pq} f^q_p e^p_q + \frac{1}{4}\sum_{pqrs} \bar{g}^{rs}_{pq} e^{pq}_{rs} = H - E_{ref} \end{aligned} \tag{5}$$

its similarity transformation admits a Baker−Campbell−Hausdorff (BCH) expansion truncating exactly after the 4-fold nested commutator.[65,78] Because all excitation operators are normal-ordered and commuting, the commutator expansion lets us reduce the Hamiltonian-excitation operator products to only those terms that are connected.[64,65] Excitation operators will only appear to the right of the Hamiltonian, and only terms where each excitation operator shares at least one index with the Hamiltonian will lead to nonzero terms in the residuals $\Omega_{\mathbf{n}}(\boldsymbol{t})$ appearing in eq 4

$$\begin{aligned} \bar{H}_N = (H_N e^T)_c = H_N + \overbrace{H_N T} + \frac{1}{2!}\overbrace{H_N TT} \\ + \frac{1}{3!}\overbrace{H_N TTT} + \frac{1}{4!}\overbrace{H_N TTTT}. \end{aligned} \tag{6}$$

Moreover, by virtue of Wick's theorem,[59,66] the products of normal-ordered strings appearing in the connected expansion will still be expressed as normal-ordered strings, further simplifying the algebra. The requirement of shared indices between the Hamiltonian and cluster coefficients enables the resulting equations to be solved via a series of tensor contractions between multi-index quantities: the sought-after cluster amplitudes and the molecular one- and two-electron integrals. The iterative process required to solve eq 4 is highly amenable for a rapid evaluation on conventional computing architectures[79,80] but remains nontrivial to parallelize,[81] especially for higher truncation orders in the CC hierarchy.[76] A proper factorization of intermediates is essential to achieve an acceptable time to solution and memory requirements.

In recent years, some of us have been involved in developing a projector MC algorithm to obtain the CC solutions within a stochastic error bar.[82−85] The starting point, as with any projector MC method, is the imaginary time Schrödinger equation[86−88] obtained after a Wick rotation $\tau \leftarrow it$. Repeated application of the approximate linear propagator to a trial wavefunction will yield the ground-state solution

$$|\Psi(\tau + \delta\tau)\rangle = [1 - \delta\tau(H - S)]|\Psi(\tau)\rangle \tag{7}$$

where S is a free parameter that is varied to keep the normalization of $\Psi(\tau)$ approximately constant. In the CCMC and FCI quantum Monte Carlo (FCIQMC) approaches, a population of particles in Fock space represents the wavefunction and evolves according to simple rules of spawning, death, and annihilation.[82,86] For a CC Ansatz, unit particles may represent nonunit contributions to CC amplitudes by letting the intermediate normalization condition vary with the population on the reference determinant: $\langle D_0|\mathrm{CCMC}(\tau)\rangle = N_0(\tau)$. A factor of $\frac{1}{N_0(\tau)}$ is removed from the definition of $T(\tau)$, and this determines the granularity of amplitude representation: amplitude values smaller than $\frac{1}{N_0(\tau)}$ are stochastically rounded during the calculation, *vide infra*. To avoid confusion, we denote the so-modified cluster operators and amplitudes as T' and $t'_{\mathbf{n}}$, respectively; therefore, $|\mathrm{CCMC}\rangle = N_0 e^{T'/N_0}|D_0\rangle$. Thus, in the unlinked formulation first put forward by Thom,[82] the dynamic equation for the amplitudes becomes

$$t'_{\mathbf{n}} \rightarrow t'_{\mathbf{n}} - \delta\tau\langle D_0|\tau^\dagger_{\mathbf{n}}[H - S]|\mathrm{CCMC}\rangle \tag{8}$$

where we have dropped the τ dependence for clarity. CCMC is fully general with respect to the truncation level in the cluster operator and sidesteps the need to store a full representation of the wavefunction at any point. CCMC should allow for the effective solution of the CC equations with a much reduced memory cost, as previously realized in the FCIQMC method.[86,89−91] However, while various cases demonstrate memory cost reduction, especially in the presence of weak correlation,[92] the corresponding increase in computational cost was large even by the standards of projector MC methods and modifications used in related approaches, such as the initiator approximation,[89] proved comparatively ineffective.[83]

Combination with the linked CC formulation seems to be one possible remedy for these issues and is furthermore the basis for decades of theoretical and implementation work in the deterministic community. Franklin et al.[84] have discussed a CCMC algorithm to sample eq 4 using the update step

$$t'_{\mathbf{n}} \rightarrow t'_{\mathbf{n}} - \delta\tau N_0\langle D_0|\tau^\dagger_{\mathbf{n}}\bar{H}|D_0\rangle \qquad (|D_{\mathbf{n}}\rangle \neq |D_0\rangle) \tag{9a}$$

$$N_0 \rightarrow N_0 - \delta\tau N_0\langle D_0|\bar{H} - S|D_0\rangle \tag{9b}$$

The authors however noted that the use of the similarity-transformed Hamiltonian required an *ad hoc* modification

$$t'_{\mathbf{n}} \rightarrow t'_{\mathbf{n}} - \delta\tau N_0\langle D_0|\tau^\dagger_{\mathbf{n}}[\bar{H} - E_{CC}]|D_0\rangle - \delta\tau(E_{CC} - S)t_{\mathbf{n}} \tag{10}$$

to deal with convergence issues with the projected energy prior to the initialization of population control. In addition, due to evaluation of $\bar{H}$ via the commutator expansion of the bare Hamiltonian, rather than the sum of connected Hamiltonian-excitation operator products (eq 6), some disconnected terms were included. These extraneous terms in the algorithm of Franklin et al.[84] have been observed to correctly cancel out on average but render unnecessarily complex the sampling of connected contributions only. Eventually, it is difficult to

DOI: 10.1021/acs.jpclett.9b00067
J. Phys. Chem. Lett. 2019, 10, 925−935

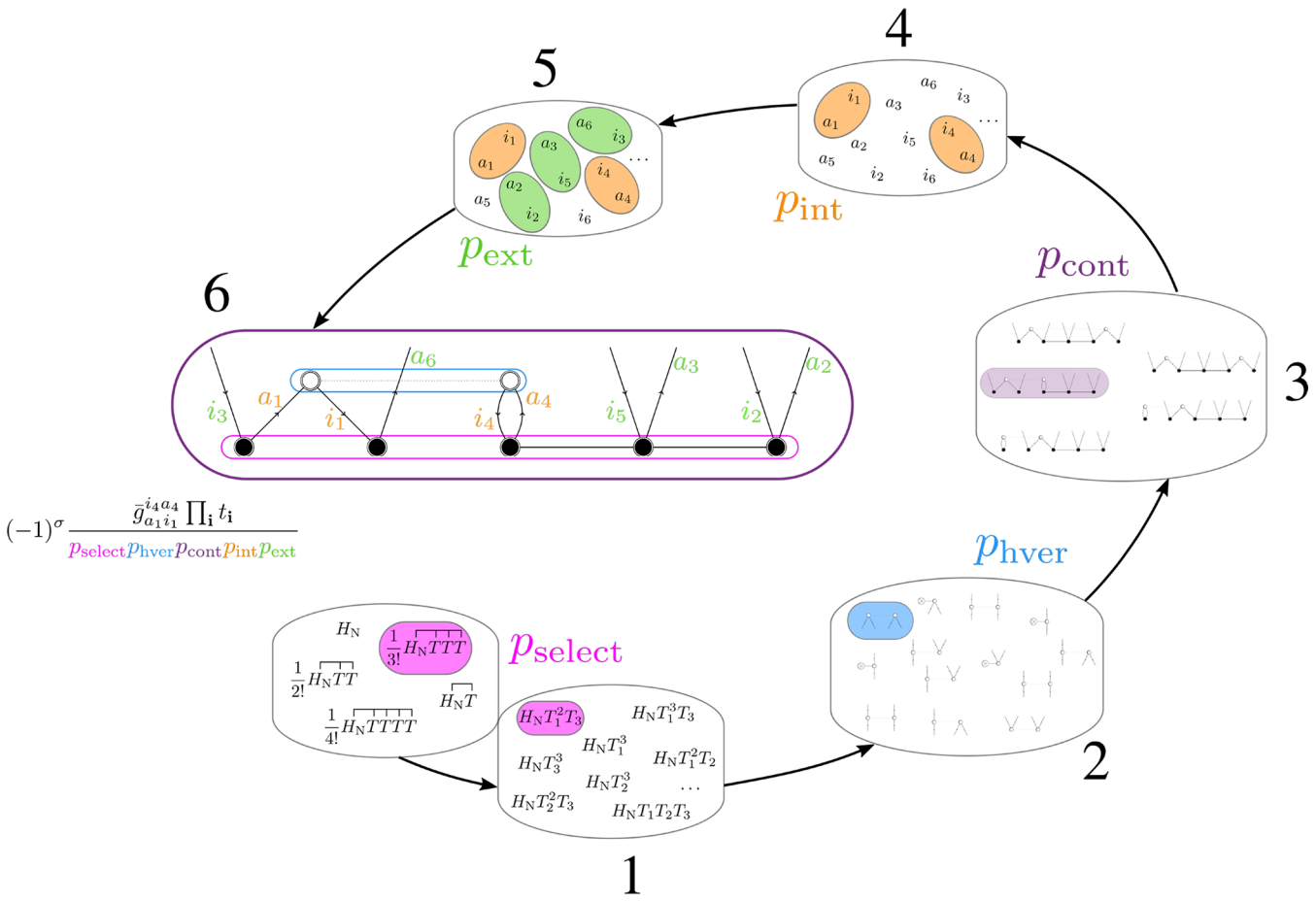

Figure 1. Graphical depiction of the diagCCMC algorithm. This example shows the steps involved in the generation of one of the possible diagrams contributing to the T_3 equations.

develop stochastic counterparts to approximations, such as the CCn hierarchy,[93,94] proposed within deterministic CC theory.

We here reconsider the implementation of the linked CCMC algorithm in light of the diagrammatic techniques used in deterministic CC, an approach we name diagrammatic coupled cluster Monte Carlo (diagCCMC). The update equation can be easily derived as a finite difference approximation to the exact imaginary time dynamics of the CC wavefunction under the assumption of constant intermediate normalization

$$t_{\mathbf{n}}(\tau + \delta\tau) = t_{\mathbf{n}}(\tau) - \delta\tau \langle D_0 | \tau_{\mathbf{n}}^{\dagger} \bar{H}_{\mathrm{N}}(\tau) | D_0 \rangle \tag{11}$$

This has been noted elsewhere,[95] and we will discuss its implications in greater detail in a subsequent communication,[96] but for now, it will suffice to observe that because this is a projector MC approach it will eventually converge to the lowest-energy solution of the CC equations. The existence of multiple solutions to the nonlinear CC equations is well-documented,[97−99] and a projector MC approach could result in a different solution to the CC equations than the one found via a deterministic procedure, where iteration stabilizes upon whichever solution is approached first from a given starting point. In practice, a difference is only observed if a highly truncated form of CC has been applied inappropriately to a system and even then only in the worst cases.

The second term on the right-hand side is the contribution to the CC vector function $\Omega_{\mathbf{n}}(\boldsymbol{t})$ resulting from the projection upon the determinant $|D_{\mathbf{n}}\rangle$ and is representable as a finite sum of enumerable diagrams. Thus, at each iteration, we wish to randomly select n_{a} diagrams from $\langle D_0 | \tau_{\mathbf{n}}^{\dagger} \bar{H}_{\mathrm{N}} | D_0 \rangle$. Each of these will be in the form of an excitation operator, $\tau_{\mathbf{i}}$, and corresponding weight, $w_{\mathbf{i}}$, selected with some known, normalized probability, p_{diagram}, such that we expect to select any given contributing diagram $p_{\text{diagram}} \times n_{\mathrm{a}}$ times at each iteration. As by construction $\langle D_0 | \tau_{\mathbf{j}}^{\dagger} \tau_{\mathbf{i}} | D_0 \rangle = \delta_{\mathbf{ij}}$, a selected term can be found to contribute to the update of a single coefficient with no additional sign considerations. Rather than explicitly introduce a particulate representation of the coefficients, as in FCIQMC and previous CCMC approaches, we stochastically round all coefficients $t_{\mathbf{n}}$ with magnitude below some strictly positive granularity parameter Δ. If $|t_{\mathbf{n}}| < \Delta$, then $|t_{\mathbf{n}}|$ is rediscretized to either Δ (with probability $\left|\frac{t_{\mathbf{n}}}{\Delta}\right|$) or 0 (with probability $1 - \left|\frac{t_{\mathbf{n}}}{\Delta}\right|$).[96,100] This can be shown to be equivalent to a representation with unit particles and constant intermediate normalization $\frac{1}{\Delta}$.

We perform diagram selection by reading off terms from right to left in $\langle D_0 | \tau_{\mathbf{n}}^{\dagger} \bar{H}_{\mathrm{N}} | D_0 \rangle$:

1. Select a random cluster of excitation operators with probability p_{select} utilizing the even selection scheme[85] restricted to clusters of at most four excitation operators. This corresponds to simultaneously selecting a term in the BCH expansion (eq 6) and the excitation level of each excitation operator in the commutator.

DOI: 10.1021/acs.jpclett.9b00067
J. Phys. Chem. Lett. 2019, 10, 925−935

2. Select 1 of the 13 possible H_N vertices[64,65] with some probability p_{hvertex}.
3. Select the contraction pattern of the chosen cluster and Hamiltonian vertex. This identifies a specific Kucharski–Bartlett sign sequence[64,65,67] for the diagram we are considering and which excitation operators are associated with which term within the sign sequence with probability p_{contract}.
4. Select which indices of each excitation operator will be contracted with the Hamiltonian vertex. Having selected the contraction pattern, this is a matter of simple combinatorics, with a given set of indices selected with probability p_{internal}.
5. Select the external indices of the Hamiltonian vertex with probability p_{external}.
6. Evaluate the index of the resulting projection determinant in the update step, i.e., $\langle D_0|\tau_{\mathbf{n}}^{\dagger}$, and the diagrammatic amplitude including all parity factors.

This obtains a single specific diagram with probability

$$p_{\text{diagram}} = p_{\text{select}} p_{\text{hver}} p_{\text{cont}} p_{\text{int}} p_{\text{ext}} \tag{12}$$

where the obvious abbreviations have been used to refer to each of the previously stated probabilities. These are conditional probabilities as the various events leading to the computed p_{diagram} are not independent. This procedure to select diagrams can be visualized as graphically building the diagram bottom-up; see Figure 1.

To evaluate the contribution of a selected diagram to our propagation, we slightly modify the standard rules of diagrammatic interpretation. Instead of summing over all indices, and thus having to correct for any potential double counting, our algorithm selects a specific diagram along with a specific set of indices for all lines.

To ensure proper normalization of our sampling probability, we require there be only a single way to select diagrams related by

- The antipermutation of antisymmetrised Goldstone vertex indices.
- The antipermutation of cluster operator particle or hole indices.
- The commutation of cluster operators.

All these modifications can be viewed as replacing sums $\frac{1}{2}\sum_{ij}$ with $\sum_{i>j}+\frac{1}{2}\delta_{ij}$. In the first two cases, summation runs over equivalent indices and the $i = j$ term must be zero, while in the third case summation runs over excitation operators and the $i = j$ term corresponds to a diagram with additional symmetry that as such must be treated more carefully to ensure unique selection of a Kucharski–Bartlett sign sequence.[64,65,67] Specifically, we do not require an additional factor of $\frac{1}{2}$ for

- each pair of equivalent internal or external lines
- two cluster operators of the same rank but with different specific indices, provided they have a well-determined ordering on selection.

Additionally, to include the effect of permutation operators $\hat{P}$ for inequivalent external lines, we must permute the hole and particle indices of a resulting excitation operator to a unique antisymmetrized ordering for storage. This ensures proper cancellation between all equivalent orderings, which could otherwise differ due to the stochastic sampling. Eventually, the amplitude of the contribution of the selected diagram, w_{diagram}, is given as the product of the cluster amplitude, $w_{\text{clus}} = \prod_i t_i$, and Hamiltonian element, w_{hamil}, with appropriately determined parity $(-1)^{\sigma}$. The overall contribution of a single selected diagram to the coefficient $t_{\mathbf{n}}$ determined by the open lines of the diagram will be

$$\frac{w_{\text{diagram}}}{p_{\text{diagram}}} = \frac{(-1)^{\sigma} w_{\text{clus}} w_{\text{hamil}}}{p_{\text{select}} p_{\text{hver}} p_{\text{cont}} p_{\text{int}} p_{\text{ext}}} \tag{13}$$

Wherever possible we aspire to have $p_{\text{diagram}} \propto |w_{\text{diagram}}|$.[85]

We will now demonstrate the ability of diagCCMC to recover energies at high levels of CC theory on the nitrogen molecule in a stretched geometry ($r_{\text{NN}} = 3.6\,a_0$). It has previously been shown that connected contributions up to hextuples are vital to obtaining high accuracy for this system.[101] Correlation energies for a range of basis sets and truncation levels are reported in Table 1, showing agreement within error bars with deterministic results[102] and the existing literature in all but the most extreme cases, where convergence to a different solution is observed as noted previously.

Table 1. Correlation Energy for Different Levels of Theory and Basis Sets for N_2 with $r_{\text{NN}} = 3.6\,a_0$[a]

		STO-3G	6-31G
SD	CC	−0.589163	−0.491480
	diagCCMC	−0.799 (2)[b]	−0.4921(7)
SDT	CC	−0.589923	−0.533600
	diagCCMC	−0.6092 (8)[b]	−0.5341(9)
SDTQ	CC	−0.523049	[c]
	diagCCMC	−0.5244(9)	
SDTQ5	CC	−0.523036	[c]
	diagCCMC	−0.5249(6)	
SDTQ56	CC	−0.527863	[c]
	diagCCMC	−0.5271(8)	

[a]Molecular integrals were generated in FCIDUMP format with the Psi4 program package.[106] The deterministic results were computed using MRCC.[102] The canonical restricted Hartree–Fock orbitals were used, giving $E_{\text{ref}} = -106.937562$ and -108.360046 E_{h} in the STO-3G and 6-31G bases, respectively. [b]In these cases, the stochastic, imaginary time propagation was found to initially converge to the conventional CC solution, before relaxing to another, lower-energy solution.[99] [c]Value not computed due to computational constraints.

We then turn our attention to test systems of beryllium and neon atoms at a variety of truncation levels. Extending these systems by introducing noninteracting replicas illustrates the behavior of our approach in the presence of locality in comparison to previous Fock space stochastic methods, namely, the original unlinked CCMC (hereafter simply referred to as CCMC) and FCIQMC.

To allow reasonable comparison among diagCCMC, CCMC, and FCIQMC, all calculations were performed with

- granularity parameter Δ equal to 10^{-4}; this is the threshold for the stochastic rounding of the cluster amplitudes
- $\delta\tau$ and n_{attempts} such that, on each iteration, a spawning event may have maximum size of 3×10^{-4}.

For CCMC and FCIQMC, this corresponds to a stable calculation with reference population of $N_0 = 10^4$ and a time step such that no spawning event produces more than three particles. CCMC and FCIQMC calculations were performed with the HANDE-QMC code[103,104] using the default, uniform

DOI: 10.1021/acs.jpclett.9b00067
J. Phys. Chem. Lett. 2019, 10, 925−935

Table 2. Correlation Energy for Different Levels of Theory Using 1, 2, and 4 Be Replicas in a cc-pVDZ Basis Set[a]

		$n_{replicas}$		
		1	2	4
SD	CCMC	−0.045032(2)	−0.09007(2)	−0.1799(1)
	diagCCMC	−0.04500(5)	−0.09011(7)	−0.1801(3)
SDT	CCMC	−0.045067(2)	−0.09012(2)	−0.18034(7)
	diagCCMC	−0.04512(4)	−0.0902(2)	−0.1802(3)
SDTQ	CCMC	−0.045070(2)	−0.09015(2)	−0.18044(9)
	diagCCMC	−0.04504(4)	−0.0902(3)	−0.1807(3)
FCI		−0.0450721(7)	−0.090151(5)	−0.18036(6)

[a]Note that for these systems CCSDTQ is equivalent to FCI. Molecular integrals were generated in FCIDUMP format with the Q-Chem program package.[105] The canonical Hartree−Fock orbitals for a single-atom calculation were used, and no spin symmetry breaking was observed, giving E_{ref} = −14.572341 E_h.

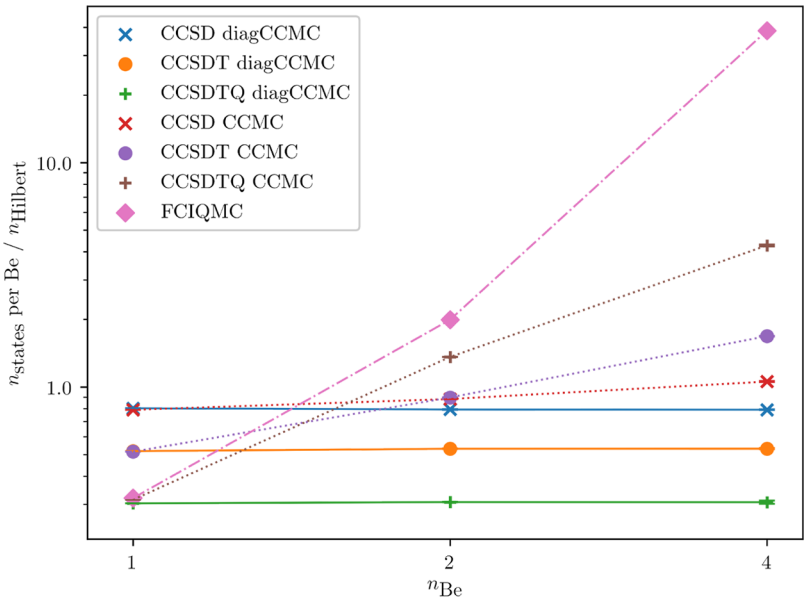

Figure 2. Ratio of states per-replica and corresponding reduced Hilbert space size for 1, 2, and 4 Be replicas in a cc-pVDZ basis set at various levels of theory. The n_{states} metric is a measure of the memory cost of the calculation. For a single Be atom the Hilbert space sizes are 121, 529, and 1093 states for CCSD, CCSDT, and CCSDTQ, respectively, and the corresponding reduced Hilbert space multiplies these values by the number of Be atoms. Note that for these systems CCSDTQ is equivalent to FCI. Solid, dotted and dash-dotted lines are used for diagCCMC, CCMC and FCIQMC results, respectively. Molecular integrals were generated in FCIDUMP format with the Q-Chem program package.[105] The canonical Hartree−Fock orbitals for a single-atom calculation were used, and no spin symmetry breaking was observed.

excitation generators. For CCMC, we adopted the even selection scheme of Scott and Thom.[85] The molecular integrals were generated in FCIDUMP format using the Q-Chem[105] and Psi4[106] quantum chemistry program packages; see the Supporting Information for more details.[107]

We report the correlation energies obtained for an isolated Be atom and the noninteracting replica systems in Table 2. We compare CC results up to and including quadruple excitations with FCIQMC. For these systems, CCSDTQ is equivalent to FCI, thus providing a good sanity check for the diagCCMC approach. In addition, results at each level of theory are expected to agree within statistical errors due to the size consistency of all considered approaches, as is observed.

In order to assess the computational performance of diagCCMC, we compare two measures of efficiency:

- $n_{attempts}/\delta\tau$, that is, the number of stochastic samples performed per unit imaginary time. This metric is a measure of the minimum CPU cost, provided that the length of propagation in imaginary time is roughly constant between approaches or equivalently a roughly constant inefficiency between the approaches.[108]
- n_{states}, that is, the number of occupied excitation operators. This metric is a measure of the minimum memory cost. For a deterministic calculation, this would amount to the Hilbert space size for the selected truncation level.

The promise of stochastic methods is to greatly reduce the cost of high-level correlated calculations by naturally exploiting the wavefunction sparsity. Figure 2 reports the ratio of n_{states} per replica and the size of the Hilbert space for an isolated atom at the given truncation level. For an isolated Be atom, the reduction in memory footprint is clearly evident: all methods compared require significantly less than the full size of the Hilbert space (ratio < 1) to successfully achieve convergence and recover the deterministic results. Unsurprisingly and correctly, diagCCMC requires the same amount of storage as its unlinked counterparts. Notice also that the ratio decreases in going from CCSD to CCSDTQ, showing how stochastic methods single out the important portions of the Hilbert space.

DOI: 10.1021/acs.jpclett.9b00067
J. Phys. Chem. Lett. 2019, 10, 925−935

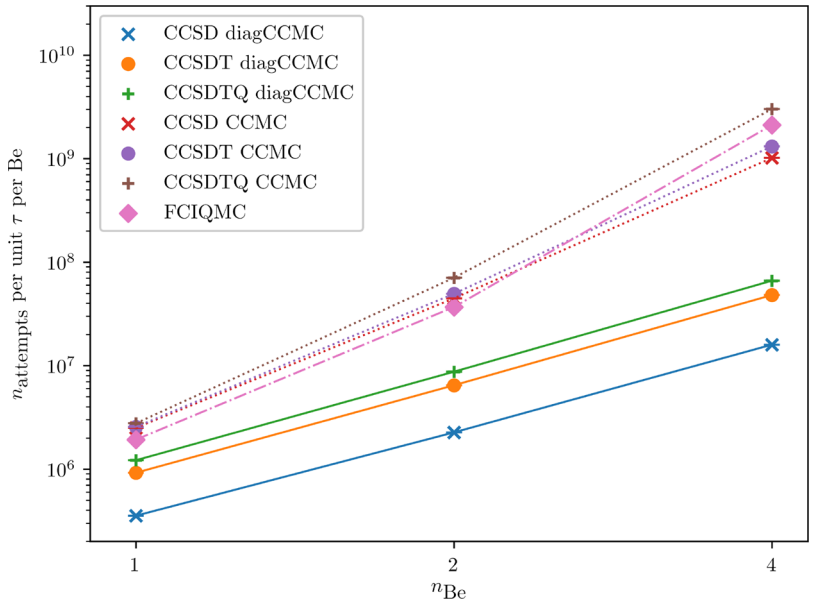

Figure 3. Number of stochastic samples performed (n_{attempts}) per unit imaginary time per replica for 1, 2, and 4 Be replicas in a cc-pVDZ basis set at various levels of theory. Assuming that the length of propagation in imaginary time is roughly constant between approaches this metric is a measure of the CPU cost of the calculation. Note that for these systems CCSDTQ is equivalent to FCI. Solid, dotted and dash-dotted lines are used for diagCCMC, CCMC and FCIQMC results, respectively. Molecular integrals were generated in FCIDUMP format with the Q-Chem program package.[105] The canonical Hartree−Fock orbitals for a single-atom calculation were used, and no spin symmetry breaking was observed.

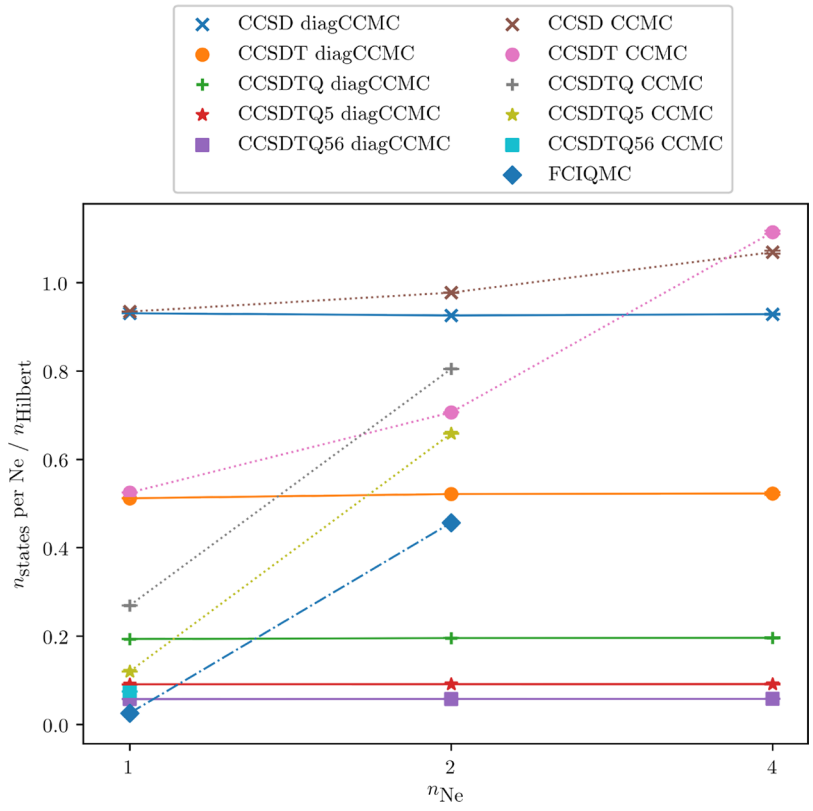

Figure 4. Ratio of states per replica and corresponding reduced Hilbert space size for 1, 2, and 4 Ne replicas in a cc-pVDZ basis set at various levels of theory. The n_{states} metric is a measure of the memory cost of the calculation. For a single Ne atom, the Hilbert space sizes are 393, 4647, 30861, 116129, 265790, and 502099 for CCSD, CCSDT, CCSDTQ, CCSDTQ5, CCSDTQ56, and FCI, respectively, and the corresponding reduced Hilbert space multiplies these values by the number of Ne atoms. Solid, dotted, and dashed−dotted lines are used for diagCCMC, CCMC, and FCIQMC results, respectively. Molecular integrals were generated in FCIDUMP format with the Q-Chem program package.[105] The canonical restricted Hartree−Fock orbitals for a single-atom calculation were used.

For perfectly local systems, such as the noninteracting two- and four-atom replicas, one also expects the number of states per replica to roughly stay constant. This expectation stems from the linked diagram theorem[65] and is met by the diagCCMC

DOI: 10.1021/acs.jpclett.9b00067
J. Phys. Chem. Lett. 2019, 10, 925−935

Table 3. Correlation Energy for Different Levels of Theory Using 1, 2, and 4 Ne Replicas in a cc-pVDZ Basis Set[a]

		$n_{replicas}$		
		1	2	4
SD	CCMC	−0.190865(3)	−0.38172(3)	−0.7633(2)
	diagCCMC	−0.19094(5)	−0.3817(1)	−0.7641(5)
	CC	−0.190861	−0.381723[c]	−0.763446[c]
SDT	CCMC	−0.191951(4)	−0.38389(4)	−0.7676(3)
	diagCCMC	−0.19185(10)	−0.3839(2)	−0.7685(7)
	CC	−0.191945	−0.383891[c]	−0.767781[c]
SDTQ	CCMC	−0.192092(4)	−0.38418(6)	[b]
	diagCCMC	−0.1924(1)	−0.3843(6)	−0.7668(7)
	CC	−0.192095	−0.384191[c]	−0.768382[c]
SDTQ5	CCMC	−0.192103(4)	−0.38436(9)	[b]
	diagCCMC	−0.1924(2)	−0.3840(5)	−0.7686(5)
	CC	−0.192106	−0.384212[c]	−0.768424[c]
SDTQ56	CCMC	−0.192119(5)	[b]	[b]
	diagCCMC	−0.1919(1)	−0.3846(6)	−0.7691(5)
	CC	−0.192106	−0.384211[c]	−0.768422[c]
FCI		−0.192106(5)	[b]	[b]

[a]Molecular integrals were generated in FCIDUMP format with the Psi4 program package[106] and exact CC results obtained using MRCC.[102] The canonical Hartree−Fock orbitals for a single-atom calculation were used, and no spin symmetry breaking was observed, giving E_{ref} = −128.488776 E_h. [b]Value not computed due to computational constraints. [c]Value obtained as a multiple of the single-atom result for comparison.

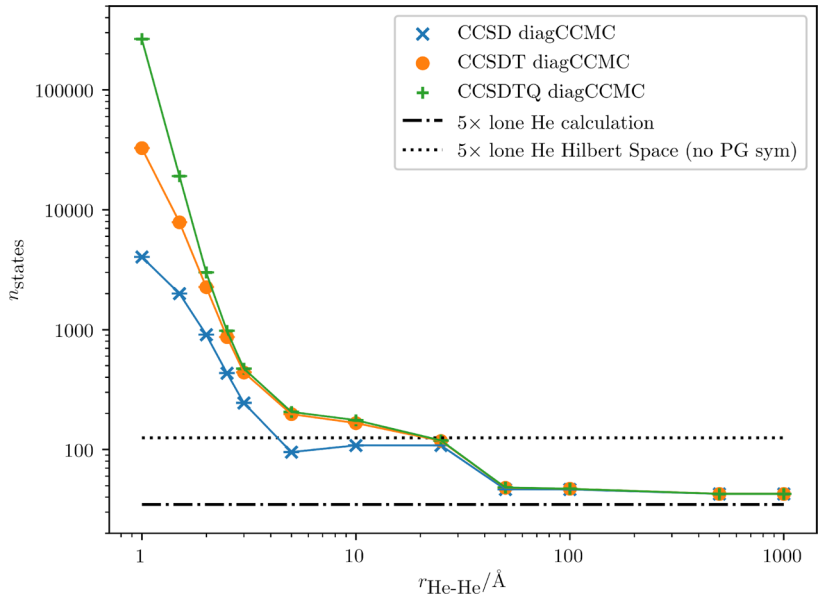

Figure 5. Number of states (n_{states}) for a line of five He atoms in a diagCCMC calculation at the CCSD, CCSDT, and CCSDTQ levels of theory. The n_{states} metric is a measure of the memory cost of the calculation. Molecular integrals were generated in FCIDUMP format with the Psi4 program package.[106] Localized orbitals were used: starting from the restricted Hartree−Fock canonical orbitals, the Foster−Boys[109] and the Pipek−Mezey[110] algorithms were used for the occupied and virtual subspaces, respectively. For CCSD, we report 5× the Hilbert space size and diagCCMC average memory cost for a single He atom using dashed−dotted and dotted horizontal lines, respectively.

approach where at each iteration only connected diagrams are sampled. The same is, quite emphatically, not true for either FCIQMC or CCMC: the number of states per replica approaches and surpasses the size of the single-atom Hilbert space.

In Figure 3, we can see that diagCCMC outperforms each of the corresponding CCMC approaches also when estimating the CPU cost of the calculations on the Be systems considered here. It is particularly striking to note the order of magnitude difference between the diagrammatic and unlinked approaches at the CCSD level of theory even for this tiny system.

The same observation also holds true for higher orders of CC theory, as can clearly be seen from Figure 4 where we plot the n_{states} metric for an isolated Ne atom and its corresponding two- and four-atom noninteracting replicas system. Table 3 reports the correlation energies per replica for a system of noninteracting Ne atoms. diagCCMC affords calculations practically at constant memory cost per replica, in contrast with CCMC for which the increasing cost exceeded available computational resources for the higher-order excitations.

Finally, we studied the dissociation of a chain of five helium atoms as an example of an interacting system. The diagrammatic algorithm shows favorable CPU and memory

DOI: 10.1021/acs.jpclett.9b00067
J. Phys. Chem. Lett. 2019, 10, 925−935

cost for noninteracting systems, further suggesting that it might also straightforwardly leverage localization in the orbital space to achieve reduced cost for calculations on interacting systems. As a preliminary test for this conjecture, Figure 5 shows the memory cost for the dissociation curve of an interacting chain of five helium atoms. We localized the occupied and virtual orbital sets with the Foster−Boys[109] and the Pipek−Mezey[110] criteria, respectively. We compare the n_{states} metric with the memory cost at the dissociation limit for a deterministic and a diagCCMC CCSD calculation. The former (dotted line) is the maximum memory cost for performing CCSD calculations on the isolated atoms: below it, the cost is comparable to that for a wavefunction with excitations localized to each He atom. The onset of such behavior is evident from Figure 5, which also shows the recovery of the noninteracting limit at large separations.

In conclusion, we have described a stochastic realization of linked CC theory that fully exploits the connectedness of the similarity-transformed Hamiltonian, as exemplified in the diagrammatic expansion of the CC equations. Our stochastic diagrammatic implementation avoids the computational and memory cost issues associated with deterministic and unlinked stochastic approaches by generating diagrams on-the-fly and accumulating the corresponding amplitudes. Finally, we have shown how the stochastic and deterministic implementations can be rationalized within the same framework. This bridges the existing gap between the two strategies: by clearing possible misunderstandings on how and why stochastic methods work and enabling future cross-fertilization.

AUTHOR INFORMATION

Corresponding Authors

*E-mail: cjcargillscott@gmail.com.
*E-mail: roberto.d.remigio@uit.no.

ORCID

Charles J. C. Scott: 0000-0001-9277-8327
Roberto Di Remigio: 0000-0002-5452-9239
T. Daniel Crawford: 0000-0002-7961-7016
Alex J. W. Thom: 0000-0002-2417-7869

Notes

The authors declare no competing financial interest.

Additional data related to this publication, including a copy of the diagCCMC code, raw and analyzed data files, and analysis scripts, are available at the University of Cambridge data repository https://doi.org/10.17863/CAM.34952 and https://doi.org/10.17863/CAM.36097. We used the gold-stone LaTeX package, available on GitHub https://github.com/avcopan/styfiles, to draw the coupled cluster diagrams. We used matplotlib for all of the plots in the paper.[111]

ACKNOWLEDGMENTS

C.J.C.S. is grateful to the Sims Fund for a studentship and A.J.W.T. to the Royal Society for a University Research Fellowship under Grant Nos. UF110161 and UF160398. Both are grateful for support under ARCHER Leadership Project Grant e507. R.D.R. acknowledges partial support by the Research Council of Norway through its Centres of Excellence scheme, Project Number 262695, and through its Mobility Grant scheme, Project Number 261873. R.D.R. is also grateful to the Norwegian Supercomputer Program through a grant for computer time (Grant No. NN4654K). T.D.C. was supported by Grants CHE-1465149 and ACI-1450169 from the U.S. National Science Foundation.

REFERENCES

(1) Pulay, P. Localizability of dynamic electron correlation. *Chem. Phys. Lett.* **1983**, *100*, 151−154.
(2) Stoll, H. On the correlation energy of graphite. *J. Chem. Phys.* **1992**, *97*, 8449−8454.
(3) Saebo, S.; Pulay, P. Local Treatment of Electron Correlation. *Annu. Rev. Phys. Chem.* **1993**, *44*, 213−236.
(4) Hampel, C.; Werner, H.-J. Local treatment of electron correlation in coupled cluster theory. *J. Chem. Phys.* **1996**, *104*, 6286−6297.
(5) Schütz, M.; Hetzer, G.; Werner, H.-J. Low-order scaling local electron correlation methods. I. Linear scaling local MP2. *J. Chem. Phys.* **1999**, *111*, 5691−5705.
(6) Schütz, M.; Werner, H.-J. Local perturbative triples correction (T) with linear cost scaling. *Chem. Phys. Lett.* **2000**, *318*, 370−378.
(7) Schütz, M. Low-order scaling local electron correlation methods. III. Linear scaling local perturbative triples correction (T). *J. Chem. Phys.* **2000**, *113*, 9986−10001.
(8) Schütz, M.; Werner, H.-J. Low-order scaling local electron correlation methods. IV. Linear scaling local coupled-cluster (LCCSD). *J. Chem. Phys.* **2001**, *114*, 661−681.
(9) Schütz, M. Low-order scaling local electron correlation methods. V. Connected triples beyond (T): Linear scaling local CCSDT-1b. *J. Chem. Phys.* **2002**, *116*, 8772−8785.
(10) Mata, R. A.; Werner, H.-J. Local correlation methods with a natural localized molecular orbital basis. *Mol. Phys.* **2007**, *105*, 2753−2761.
(11) Taube, A. G.; Bartlett, R. J. Frozen natural orbital coupled-cluster theory: Forces and application to decomposition of nitro-ethane. *J. Chem. Phys.* **2008**, *128*, 164101.
(12) Li, W.; Piecuch, P.; Gour, J. R.; Li, S. Local correlation calculations using standard and renormalized coupled-cluster approaches. *J. Chem. Phys.* **2009**, *131*, 114109.
(13) Neese, F.; Hansen, A.; Liakos, D. G. Efficient and accurate approximations to the local coupled cluster singles doubles method using a truncated pair natural orbital basis. *J. Chem. Phys.* **2009**, *131*, 064103.
(14) Neese, F.; Wennmohs, F.; Hansen, A. Efficient and accurate local approximations to coupled-electron pair approaches: An attempt to revive the pair natural orbital method. *J. Chem. Phys.* **2009**, *130*, 114108.
(15) Piecuch, P. Active-space coupled-cluster methods. *Mol. Phys.* **2010**, *108*, 2987−3015.
(16) Li, W.; Piecuch, P. Improved Design of Orbital Domains within the Cluster-in-Molecule Local Correlation Framework: Single-Environment Cluster-in-Molecule Ansatz and Its Application to Local Coupled-Cluster Approach with Singles and Doubles. *J. Phys. Chem. A* **2010**, *114*, 8644−8657.
(17) Liakos, D. G.; Hansen, A.; Neese, F. Weak Molecular Interactions with Parellel Implementations of the Local Pair Natural Orbital Coupled Pair and Coupled Cluster Methods. *J. Chem. Theory Comput.* **2011**, *7*, 76−87.
(18) Tew, D. P.; Helmich, B.; Hättig, C. Local explicitly correlated second-order Møller-Plesset perturbation theory with pair natural orbtials. *J. Chem. Phys.* **2011**, *135*, 074107.
(19) Yang, J.; Kurashige, Y.; Manby, F. R.; Chan, G. K. L. Tensor factorizations of local second-order Møller-Plesset theory. *J. Chem. Phys.* **2011**, *134*, 044123.
(20) Yang, J.; Chan, G. K.-L.; Manby, F. R.; Schütz, M.; Werner, H.-J. The orbital-specific-virtual local coupled cluster singles and doubles method. *J. Chem. Phys.* **2012**, *136*, 144105.
(21) Liakos, D. G.; Neese, F. Improved correlation energy extrapolation schemes based on local pair natural orbital methods. *J. Phys. Chem. A* **2012**, *116*, 4801−4816.

DOI: 10.1021/acs.jpclett.9b00067
J. Phys. Chem. Lett. 2019, 10, 925−935

(22) Hättig, C.; Tew, D. P.; Helmich, B. Local explicitly correlated second- and third-order Møller-Plesset perturbation theory with pair natual orbitals. *J. Chem. Phys.* **2012**, *136*, 204105.
(23) Krause, C.; Werner, H.-J. Comparison of explicitly correlated local coupled-cluster methods with various choices of virtual orbitals. *Phys. Chem. Chem. Phys.* **2012**, *14*, 7591−7604.
(24) Masur, O.; Usvyat, D.; Schütz, M. Efficient and accurate treatment of weak pairs in local CCSD(T) calculations. *J. Chem. Phys.* **2013**, *139*, 164116.
(25) Riplinger, C.; Neese, F. An efficient and near linear scaling pair natural orbital based local coupled cluster method. *J. Chem. Phys.* **2013**, *138*, 034106.
(26) Riplinger, C.; Sandhoefer, B.; Hansen, A.; Neese, F. Natural triple excitations in local coupled cluster calculations with pair natural orbitals. *J. Chem. Phys.* **2013**, *139*, 134101.
(27) Werner, H.-J.; Knizia, G.; Krause, C.; Schwilk, M.; Dornbach, M. Scalable Electron Correlation Methods I.: PNO-LMP2 with Linear Scaling in the Molecular Size and Near-Inverse-Linear Scaling in the Number of Processors. *J. Chem. Theory Comput.* **2015**, *11*, 484−507.
(28) Liakos, D. G.; Sparta, M.; Kesharwani, M. K.; Martin, J. M. L.; Neese, F. Exploring the Accuracy Limits of Local Pair Natural Orbital Coupled-Cluster Theory. *J. Chem. Theory Comput.* **2015**, *11*, 1525−1539.
(29) Riplinger, C.; Pinski, P.; Becker, U.; Valeev, E. F.; Neese, F. Sparse maps−A systematic infrastructure for reduced-scaling electronic structure methods. II. Linear scaling domain based pair natural orbital coupled cluster theory. *J. Chem. Phys.* **2016**, *144*, 024109.
(30) Pavosevic, F.; Pinski, P.; Riplinger, C.; Neese, F.; Valeev, E. F. SparseMaps-A systematic infrastructure for reduced-scaling electronic structure methods. IV. Linear-scaling second-order explicitly correlated energy with pair natural orbitals. *J. Chem. Phys.* **2016**, *144*, 144109.
(31) Pavosevic, F.; Peng, C.; Pinski, P.; Riplinger, C.; Neese, F.; Valeev, E. F. SparseMaps-A systematic infrastructure for reduced scaling electronic structure methods. V. Linear scaling explicitly correlated coupled-cluster method with pair natural orbitals. *J. Chem. Phys.* **2017**, *146*, 174108.
(32) Saitow, M.; Becker, U.; Riplinger, C.; Valeev, E. F.; Neese, F. A new near-linear scaling, efficient and accurate, open-shell domain-based local pair natural orbital coupled cluster singles and doubles theory. *J. Chem. Phys.* **2017**, *146*, 164105.
(33) Guo, Y.; Riplinger, C.; Becker, U.; Liakos, D. G.; Minenkov, Y.; Cavallo, L.; Neese, F. Communication: An improved linear scaling perturbative triples correction for the domain based local pair-natural orbital based singles and doubles coupled cluster method [DLPNO-CCSD(T)]. *J. Chem. Phys.* **2018**, *148*, 011101.
(34) Yang, J.; Chan, G. K.-L.; Manby, F. R.; Schütz, M.; Werner, H.-J. The orbital-specific-virtual local coupled cluster singles and doubles method. *J. Chem. Phys.* **2012**, *136*, 144105.
(35) Schwilk, M.; Usvyat, D.; Werner, H.-J. Communication: Improved pair approximations in local coupled-cluster methods. *J. Chem. Phys.* **2015**, *142*, 121102.
(36) Ma, Q.; Schwilk, M.; Köppl, C.; Werner, H.-J. Scalable Electron Correlation Methods. 4. Parallel Explicitly Correlated Local Coupled Cluster with Pair Natural Orbitals (PNO-LCCSD-F12). *J. Chem. Theory Comput.* **2017**, *13*, 4871−4896.
(37) Schwilk, M.; Ma, Q.; Köppl, C.; Werner, H.-J. Scalable Electron Correlation Methods. 3. Efficient and Accurate Parallel Local Coupled Cluster with Pair Natural Orbitals (PNO-LCCSD). *J. Chem. Theory Comput.* **2017**, *13*, 3650−3675.
(38) Ma, Q.; Werner, H.-J. Scalable Electron Correlation Methods. 5. Parallel Perturbative Triples Correction for Explicitly Correlated Local Coupled Cluster with Pair Natural Orbitals. *J. Chem. Theory Comput.* **2018**, *14*, 198−215.
(39) Kitaura, K.; Ikeo, E.; Asada, T.; Nakano, T.; Uebayasi, M. Fragment molecular orbital method: an approximate computational method for large molecules. *Chem. Phys. Lett.* **1999**, *313*, 701−706.
(40) Li, W.; Li, S. Divide-and-conquer local correlation approach to the correlation energy of large molecules. *J. Chem. Phys.* **2004**, *121*, 6649−6657.
(41) Fedorov, D. G.; Kitaura, K. Coupled-cluster theory based upon the fragment molecular-orbital method. *J. Chem. Phys.* **2005**, *123*, 134103.
(42) Li, S.; Shen, J.; Li, W.; Jiang, Y. An efficient implementation of the "cluster-in-molecule" approach for local electron correlation calculations. *J. Chem. Phys.* **2006**, *125*, 074109.
(43) Li, W.; Piecuch, P.; Gour, J. R. In *Theory and Applications of Computational Chemistry*; Wei, D. Q., Wang, X. J., Eds.; AIP Conference Proceedings; American Institute of Physics: Melville, NY, 2009; Vol. *1102*; pp 68−113.
(44) Stoll, H. Can incremental expansions cope with high-order coupled-cluster contributions? *Mol. Phys.* **2010**, *108*, 243−248.
(45) Friedrich, J.; Dolg, M. Fully automated incremental evaluation of MP2 and CCSD(T) energies: application to water clusters. *J. Chem. Theory Comput.* **2009**, *5*, 287−294.
(46) Ziółkowski, M.; Jansík, B.; Kjaergaard, T.; Jørgensen, P. Linear scaling coupled cluster method with correlation energy based error control. *J. Chem. Phys.* **2010**, *133*, 014107.
(47) Kristensen, K.; Ziółkowski, M.; Jansík, B.; Kjærgaard, T.; Jørgensen, P. A Locality Analysis of the Divide-Expand-Consolidate Coupled Cluster Amplitude Equations. *J. Chem. Theory Comput.* **2011**, *7*, 1677−1694.
(48) Rolik, Z.; Kállay, M. A general-order local coupled-cluster method based on the cluster-in-molecule approach. *J. Chem. Phys.* **2011**, *135*, 104111.
(49) Høyvik, I.-M.; Kristensen, K.; Jansik, B.; Jørgensen, P. The divide-expand-consolidate family of coupled cluster methods: numerical illustrations using second order Møller-Plesset perturbation theory. *J. Chem. Phys.* **2012**, *136*, 014105.
(50) Gordon, M. S.; Fedorov, D. G.; Pruitt, S. R.; Slipchenko, L. V. Fragmentation methods: a route to accurate calculations on large systems. *Chem. Rev.* **2012**, *112*, 632−672.
(51) Eriksen, J. J.; Baudin, P.; Ettenhuber, P.; Kristensen, K.; Kjærgaard, T.; Jørgensen, P. Linear-Scaling Coupled Cluster with Perturbative Triple Excitations: The Divide-Expand-Consolidate CCSD(T) Model. *J. Chem. Theory Comput.* **2015**, *11*, 2984−2993.
(52) Kinoshita, T.; Hino, O.; Bartlett, R. Singular value decomposition approach for the approximate coupled-cluster method. *J. Chem. Phys.* **2003**, *119*, 7756−7762.
(53) Hättig, C.; Weigend, F. CC2 excitation energy calculations on large molecules using the resolution of the identity approximation. *J. Chem. Phys.* **2000**, *113*, 5154−5161.
(54) Hättig, C.; Köhn, A. Transition moments and excited-state first-order properties in the coupled-cluster model CC2 using the resolution-of-the-identity approximation. *J. Chem. Phys.* **2002**, *117*, 6939−6951.
(55) Koch, H.; Sanchez de Merás, A. M. J.; Pedersen, T. B. Reduced scaling in electronic structure calculations using Cholesky decompositions. *J. Chem. Phys.* **2003**, *118*, 9481−9484.
(56) Pedersen, T. B.; Koch, H.; Boman, L.; Sanchez de Meras, A. M. J. Origin invariant calculation of optical rotation without recourse to London orbitals. *Chem. Phys. Lett.* **2004**, *393*, 319−326.
(57) Epifanovsky, E.; Zuev, D.; Feng, X.; Khistyaev, K.; Shao, Y.; Krylov, A. I. General implementation of the resolution-of-the-identity and Cholesky representations of electron repulsion integrals within coupled-cluster and equation-of-motion methods: Theory and benchmarks. *J. Chem. Phys.* **2013**, *139*, 134105.
(58) Lehtola, S.; Tubman, N. M.; Whaley, K. B.; Head-Gordon, M. Cluster decomposition of full configuration interaction wave functions: A tool for chemical interpretation of systems with strong correlation. *J. Chem. Phys.* **2017**, *147*, 154105.
(59) Kutzelnigg, W.; Mukherjee, D. Normal order and extended Wick theorem for a multiconfiguration reference wave function. *J. Chem. Phys.* **1997**, *107*, 432.

DOI: 10.1021/acs.jpclett.9b00067
J. Phys. Chem. Lett. 2019, 10, 925−935

(60) Christiansen, O.; Jørgensen, P.; Hättig, C. Response functions from Fourier component variational perturbation theory applied to a time-averaged quasienergy. *Int. J. Quantum Chem.* **1998**, *68*, 1−52.
(61) Noga, J.; Bartlett, R. J. The full CCSDT model for molecular electronic structure. *J. Chem. Phys.* **1987**, *86*, 7041−7050.
(62) Kucharski, S. A.; Bartlett, R. J. The coupled-cluster single, double, triple, and quadruple excitation method. *J. Chem. Phys.* **1992**, *97*, 4282.
(63) Hirata, S.; Bartlett, R. J. High-order coupled-cluster calculations through connected octuple excitations. *Chem. Phys. Lett.* **2000**, *321*, 216−224.
(64) Crawford, T. D.; Schaefer, H. F., III An introduction to coupled cluster theory for computational chemists. *Rev. Comput. Chem.* **2007**, *14*, 33−136.
(65) Shavitt, I.; Bartlett, R. J. *Many-Body Methods in Chemistry and Physics: MBPT and Coupled-Cluster Theory*; Cambridge Molecular Science; Cambridge University Press, 2009.
(66) Wick, G. C. The Evaluation of the Collision Matrix. *Phys. Rev.* **1950**, *80*, 268.
(67) Kucharski, S. A.; Bartlett, R. J. In *Advances in Quantum Chemistry*; Löwdin, P.-O., Ed.; Academic Press, 1986; Vol. *18*; pp 281−344.
(68) Harris, F. E. Computer generation of coupled-cluster equations. *Int. J. Quantum Chem.* **1999**, *75*, 593−597.
(69) Kállay, M.; Surján, P. R. Higher excitations in coupled-cluster theory. *J. Chem. Phys.* **2001**, *115*, 2945−2954.
(70) Kállay, M.; Gauss, J. Analytic second derivatives for general coupled-cluster and configuration-interaction models. *J. Chem. Phys.* **2004**, *120*, 6841−6848.
(71) Kállay, M.; Gauss, J.; Szalay, P. G. Analytic first derivatives for general coupled-cluster and configuration interaction models. *J. Chem. Phys.* **2003**, *119*, 2991−3004.
(72) Kállay, M.; Gauss, J. Calculation of excited-state properties using general coupled-cluster and configuration-interaction models. *J. Chem. Phys.* **2004**, *121*, 9257−9269.
(73) Lyakh, D. I.; Ivanov, V. V.; Adamowicz, L. Automated generation of coupled-cluster diagrams: implementation in the multireference state-specific coupled-cluster approach with the complete-active-space reference. *J. Chem. Phys.* **2005**, *122*, 024108.
(74) Krupička, M.; Sivalingam, K.; Huntington, L.; Auer, A. A.; Neese, F. A toolchain for the automatic generation of computer codes for correlated wavefunction calculations. *J. Comput. Chem.* **2017**, *38*, 1853−1868.
(75) Matthews, D. A.; Gauss, J.; Stanton, J. F. Revisitation of Nonorthogonal Spin Adaptation in Coupled Cluster Theory. *J. Chem. Theory Comput.* **2013**, *9*, 2567−2572.
(76) Matthews, D. A.; Stanton, J. F. Non-orthogonal spin-adaptation of coupled cluster methods: A new implementation of methods including quadruple excitations. *J. Chem. Phys.* **2015**, *142*, 064108.
(77) Wang, C.; Knizia, G. A simple permutation group approach to spin-free higher-order coupled-cluster methods. *arXiv e-prints* **2018**, arXiv:1805.00565.
(78) Helgaker, T.; Jørgensen, P.; Olsen, J. *Molecular Electronic-Structure Theory*, 1st ed.; John Wiley & Sons, 2000.
(79) Stanton, J. F.; Gauss, J.; Watts, J. D.; Bartlett, R. J. A direct product decomposition approach for symmetry exploitation in many-body methods. I. Energy calculations. *J. Chem. Phys.* **1991**, *94*, 4334−4345.
(80) Gauss, J.; Stanton, J. F.; Bartlett, R. J. Coupled-cluster open-shell analytic gradients: Implementation of the direct product decomposition approach in energy gradient calculations. *J. Chem. Phys.* **1991**, *95*, 2623−2638.
(81) Peng, C.; Calvin, J. A.; Pavošević, F.; Zhang, J.; Valeev, E. F. Massively Parallel Implementation of Explicitly Correlated Coupled-Cluster Singles and Doubles Using TiledArray Framework. *J. Phys. Chem. A* **2016**, *120*, 10231−10244.
(82) Thom, A. J. W. Stochastic coupled cluster theory. *Phys. Rev. Lett.* **2010**, *105*, 263004.
(83) Spencer, J. S.; Thom, A. J. W. Developments in Stochastic Coupled Cluster Theory: The initiator approximation and application to the Uniform Electron Gas. *J. Chem. Phys.* **2016**, *144*, 084108.
(84) Franklin, R. S. T.; Spencer, J. S.; Zoccante, A.; Thom, A. J. W. Linked coupled cluster Monte Carlo. *J. Chem. Phys.* **2016**, *144*, 044111.
(85) Scott, C. J. C.; Thom, A. J. W. Stochastic coupled cluster theory: Efficient sampling of the coupled cluster expansion. *J. Chem. Phys.* **2017**, *147*, 124105.
(86) Booth, G. H.; Thom, A. J. W.; Alavi, A. Fermion monte carlo without fixed nodes: A game of life, death, and annihilation in Slater determinant space. *J. Chem. Phys.* **2009**, *131*, 054106.
(87) Foulkes, W. M. C.; Mitas, L.; Needs, R. J.; Rajagopal, G. Quantum Monte Carlo simulations of solids. *Rev. Mod. Phys.* **2001**, *73*, 33.
(88) Toulouse, J.; Assaraf, R.; Umrigar, C. J. Introduction to the variational and diffusion Monte Carlo methods. *Adv. Quantum Chem.* **2016**, *73*, 285.
(89) Cleland, D.; Booth, G. H.; Alavi, A. Communications: Survival of the fittest: Accelerating convergence in full configuration-interaction quantum Monte Carlo. *J. Chem. Phys.* **2010**, *132*, 041103.
(90) Petruzielo, F. R.; Holmes, A. A.; Changlani, H. J.; Nightingale, M. P.; Umrigar, C. J. Semistochastic projector monte carlo method. *Phys. Rev. Lett.* **2012**, *109*, 1−5.
(91) Blunt, N. S.; Smart, S. D.; Kersten, J. A. F.; Spencer, J. S.; Booth, G. H.; Alavi, A. Semi-stochastic full configuration interaction quantum Monte Carlo: Developments and application. *J. Chem. Phys.* **2015**, *142*, 184107.
(92) Neufeld, V. A.; Thom, A. J. W. A study of the dense uniform electron gas with high orders of coupled cluster. *J. Chem. Phys.* **2017**, *147*, 194105.
(93) Christiansen, O.; Koch, H.; Jørgensen, P. The second-order approximate coupled cluster singles and doubles model CC2. *Chem. Phys. Lett.* **1995**, *243*, 409−418.
(94) Koch, H.; Christiansen, O.; Jørgensen, P.; Sanchez de Merás, A. M.; Helgaker, T. The CC3 model: An iterative coupled cluster approach including connected triples. *J. Chem. Phys.* **1997**, *106*, 1808−1818.
(95) Ten-No, S. L. Multi-state effective Hamiltonian and size-consistency corrections in stochastic configuration interactions. *J. Chem. Phys.* **2017**, *147*, 244107.
(96) Scott, C. J. C.; Di Remigio, R.; Crawford, T. D.; Thom, A. J. W. Manuscript in preparation.
(97) Kowalski, K.; Jankowski, K. Full solution to the coupled-cluster equations: the H4 model. *Chem. Phys. Lett.* **1998**, *290*, 180−188.
(98) Kowalski, K.; Jankowski, K. Towards Complete Solutions to Systems of Nonlinear Equations of Many-Electron Theories. *Phys. Rev. Lett.* **1998**, *81*, 1195−1198.
(99) Piecuch, P.; Kowalski, K. *Computational Chemistry: Reviews of Current Trends*; World Scientific, 2000; pp 1−104.
(100) Overy, C.; Booth, G. H.; Blunt, N. S.; Shepherd, J. J.; Cleland, D.; Alavi, A. Unbiased reduced density matrices and electronic properties from full configuration interaction quantum Monte Carlo. *J. Chem. Phys.* **2014**, *141*, 244117.
(101) Chan, G. K.-L.; Kállay, M.; Gauss, J. State-of-the-art density matrix renormalization group and coupled cluster theory studies of the nitrogen binding curve. *J. Chem. Phys.* **2004**, *121*, 6110.
(102) (a) Kállay, M.; Rolik, Z.; Csontos, J.; Nagy, P.; Samu, G.; Mester, D.; Csóka, J.; Szabó, B.; Ladjánszki, I.; Szegedy, L.; Ladóczki, B.; Petrov, K.; Farkas, M.; Mezei, P. D.; Hégely, B. *MRCC, a quantum chemical program suite*. www.mrcc.hu (2018). (b) Rolik, Z.; Szegedy, L.; Ladjánszki, I.; Ladóczki, B.; Kállay, M. An efficient linear-scaling CCSD(T) method based on local natural orbitals. *J. Chem. Phys.* **2013**, *139*, 094105.
(103) Spencer, J. S.; Blunt, N. S.; Vigor, W. A.; Malone, F. D.; Foulkes, W. M. C.; Shepherd, J. J.; Thom, A. J. W. Open-Source Development Experiences in Scientific Software: The HANDE Quantum Monte Carlo Project. *J. Open Res. Softw.* **2015**, *3*.

DOI: 10.1021/acs.jpclett.9b00067
J. Phys. Chem. Lett. 2019, 10, 925−935

(104) Spencer, J. S.; Blunt, N. S.; Choi, S.; Etrych, J.; Filip, M.-A.; Foulkes, W. M. C.; Franklin, R. S. T.; Handley, W. J.; Malone, F. D.; Neufeld, V. A. The HANDE-QMC project: open-source stochastic quantum chemistry from the ground state up. *J. Chem. Theory Comput.* **2019**, DOI: 10.1021/acs.jctc.8b01217.
(105) Shao, Y.; Gan, Z.; Epifanovsky, E.; Gilbert, A. T. B.; Wormit, M.; Kussmann, J.; Lange, A. W.; Behn, A.; Deng, J.; Feng, X.; et al. Advances in molecular quantum chemistry contained in the Q-Chem 4 program package. *Mol. Phys.* **2015**, *113*, 184−215.
(106) Parrish, R. M.; Burns, L. A.; Smith, D. G. A.; Simmonett, A. C.; DePrince, A. E., 3rd; Hohenstein, E. G.; Bozkaya, U.; Sokolov, A. Y.; Di Remigio, R.; Richard, R. M.; et al. Psi4 1.1: An Open-Source Electronic Structure Program Emphasizing Automation, Advanced Libraries, and Interoperability. *J. Chem. Theory Comput.* **2017**, *13*, 3185−3197.
(107) Scott, C. J. C.; Di Remigio, R.; Crawford, T. D.; Thom, A. J. W. Research data supporting "Diagrammatic Coupled Cluster Monte Carlo". https://doi.org/10.17863/CAM.34952 (2019).
(108) Vigor, W. A.; Spencer, J. S.; Bearpark, M. J.; Thom, A. J. W. Understanding and improving the efficiency of full configuration interaction quantum Monte Carlo. *J. Chem. Phys.* **2016**, *144*, 094110.
(109) Foster, J. M.; Boys, S. F. Canonical Configurational Interaction Procedure. *Rev. Mod. Phys.* **1960**, *32*, 300−302.
(110) Pipek, J.; Mezey, P. G. A fast intrinsic localization procedure applicable for a b i n i t i o and semiempirical linear combination of atomic orbital wave functions. *J. Chem. Phys.* **1989**, *90*, 4916−4926.
(111) Hunter, J. D. Matplotlib: A 2D Graphics Environment. *Comput. Sci. Eng.* **2007**, *9*, 90−95.

DOI: 10.1021/acs.jpclett.9b00067
J. Phys. Chem. Lett. 2019, 10, 925−935